

El Pinacate volcanic field, Northwest Mexico: An example of a shield cluster

Campo volcánico El Pinacate, noroeste de México: Un ejemplo de un cúmulo de escudos

Edgardo Cañón-Tapia^{1,*}, Rocío A. Jacobo-Bojórquez^{1,2}

¹ CICESE- División de Ciencias de la Tierra. Carretera Ensenada-Tijuana # 3918, 22860, Ensenada Baja California, Mexico.

² College of Science, Lunar and Planetary Laboratory, The University of Arizona, USA.

* Corresponding author: (E. Cañón-Tapia) ecanon@cicese.mx

ABSTRACT

El Pinacate volcanic field, Northwest Mexico, includes a large shield volcano (Sta. Clara) and more than 400 vents, most of which are cinder cones and a few maars of Pleistocene and recent age. Previous studies of the distribution of those vents focused on the identification of preferred orientations of vent alignments, paying little attention to the identification of clusters of vents within the field. In this work several methods of spatial distribution analyses are combined together to describe the spatial structure of the distribution. As a result, four main structures are identified, each interpreted as a long-lived volcanic system that has remained active throughout the history of the volcanic activity on the region. Interaction of the axes of activity within those structures with an older listric fault that crosses the field from NW to SE is responsible for the apparent difference in distribution observed in the north and south halves of the field. Differences to the depth of the Curie isotherm also contribute to the observed differences on the vent distribution at the surface. Although the influence of tectonic stresses is very important in controlling the location of activity on this field, in this work we show that it is not necessary to invoke a change in the orientation of those stresses to explain the evolution of the region

Keywords: spatial distribution of volcanic centers, Distributed volcanism, El Pinacate, volcanic field.

RESUMEN

El campo volcánico El Pinacate, en el noroeste de México, incluye un gran volcán en escudo (Sta. Clara) y más de 400 centros eruptivos, la mayoría de los cuales son conos de ceniza con solo algunos maars, del Pleistoceno y más recientes. Estudios previos de la distribución de esos centros eruptivos han descrito su orientación preferente, prestando poca atención a la identificación de grupos. En este trabajo se combinan varios métodos de análisis para describir la estructura espacial de la distribución. Como resultado, se identifican cuatro estructuras principales, cada una interpretada como un sistema volcánico de larga vida que se ha mantenido activo a lo largo de la historia de la actividad volcánica en la región. La interacción de los ejes de actividad dentro de aquellas estructuras con una falla listrica más antigua que cruza el campo de NW a SE es responsable de la aparente diferencia en la distribución observada en las mitades norte y sur del campo. Las diferencias en la profundidad de la isoterma de Curie también contribuyen a las diferencias observadas en la distribución de los respiraderos en la superficie. Aunque la influencia de los esfuerzos tectónicos es muy importante para controlar la ubicación de la actividad en este campo, en este trabajo mostramos que no es necesario invocar un cambio en la orientación de esos esfuerzos para explicar la evolución de la región.

Palabras clave: distribución espacial de centros volcánicos, Distribución volcánica, El Pinacate, campos volcánicos.

How to cite this article:

Cañón-Tapia, E., Jacobo-Bojórquez, R.A., 2023, El Pinacate volcanic field, Northwest Mexico: An example of a shield cluster: Boletín de la Sociedad Geológica Mexicana, 75 (2), A020523. <http://dx.doi.org/10.18268/BSGM2023v75n2a020523>

Manuscript received: May 1, 2023.

Corrected manuscript received: May 9, 2023.

Manuscript accepted: May 12, 2023.

Peer Reviewing under the responsibility of Universidad Nacional Autónoma de México.

This is an open access article under the CC BY-NC-SA license (<https://creativecommons.org/licenses/by-nc-sa/4.0/>)

1. Introduction

The volcanic origin of the area surrounding El Pinacate and Santa Clara mountains, in present day Sonora, northwestern Mexico, has been known for more than 300 yrs (Ives, 1942). Modern research on El Pinacate before the 1990's has been summarized by Gutmann (2007) who also provides remarks of personal experiences that capture the difficulties faced when conducting field work on this area characterized by an arid climate, lack of roads and settlements, and some terrains of a hazardous nature. Most of those studies focused on a few specific craters such as El Tecolote, Elegante, or Cerro Colorado, or the voluminous Ives lava flow (estimated volume between 0.25 to 0.5 km³ according to Lynch, 1991), from where most estimates of age, chemical and mineral compositions and paleomagnetic signature of the entire volcanic field have been inferred (Alva Valdivia *et al.*, 2019; Gutmann, 2002; Lynch, 1991; Lynch *et al.*, 1993; Lynch, 1981; Martin and Nemeth, 2004; Rodríguez-Trejo *et al.*, 2019; Turrin *et al.*, 2008; Zawacki *et al.*, 2019). Occasionally, El Pinacate has been mentioned as part of a much broader research that compares some attributes of this field with other volcanic fields elsewhere on Earth or even in other planets (e.g., Jacobo-Bojórquez and Cañón-Tapia, 2020; Le Corvec *et al.*, 2013), or in the context of regional gravity and aeromagnetic data used to constrain crustal structure and to determine Curie temperatures (Campos-Enriquez *et al.*, 2019; Sumner, 1972). Such information has been interpreted as indicating the presence of a large subsurface body beneath the northern half of the volcanic field and of a smaller one beneath the southern half (García-Abdeslem and Calmus, 2015). The exact nature of both subsurface bodies, however, remains enigmatic.

The spatial distribution of volcanic vents in El Pinacate has been studied through several methods aimed to identify vent alignments (García-Abdeslem, 2020; Lutz and Gutmann, 1995; Wadge and Cross, 1989). In all cases a N20°W alignment has been identified, but its nature remains controversial. Other orientations have been reported,

depending on the method used for the analysis. The degree of clustering of vents also has been described (Jacobo-Bojórquez and Cañón-Tapia, 2020; Le Corvec *et al.*, 2013), but no interpretation concerning the underlying plumbing system has been drawn from such studies.

In this work we reexamine the spatial distribution of volcanic vents in El Pinacate by combining several methods of analysis aiming to identify patterns that include, but are not limited to, the identification of alignments. This approach has provided glimpses of the sub-volcanic system in other places on Earth and the Moon (Cañón-Tapia, 2021a; Cañón-Tapia, 2021b; Cañón-Tapia and Jacobo-Bojórquez, 2022).

2. Geologic setting

Morphologically, the southern part of the field is dominated by the Santa Clara volcano (Lynch, 1981). The northern half of the field is topographically lower, and has no prominent structures, although two small topographic heights can be barely identified north of Santa Clara (Figure 1). Based on the geometric characteristics and the geographic distribution of flows, Donnelly (1974) proposed the presence of three shield volcanoes in the region, but the lack of a clear topographic expression for those shields (except Santa Clara), casts doubts concerning the existence of those edifices.

Volcanism has occurred since at least 1.7 Ma (Lynch, 1981), with the youngest activity probably occurring no more than a few thousand years ago (Alva Valdivia *et al.*, 2019). Such activity has been responsible for the formation of a trachytic shield known as the Santa Clara volcano, and later for the formation of the 416 basaltic vents identified by Lutz and Gutmann (1995), all of which are thought to be monogenetic. Those monogenetic vents cover the surface of El Pinacate defining the volcanic field that is observed at present.

An hypothetical component of El Pinacate is a listric fault that may cut the field diagonally in a NW-SE direction, but geophysical studies fail

to provide concrete evidence. Lutz and Gutmann (1995) discuss such a fault based on evidence obtained outside the boundaries of the Pinacate field, associating it with the opening of the Gulf of California, therefore implying its formation ~ 5 Ma before the present. According to them, the orientation of this inferred fault presents problems concerning the orientation of N-S vent alignments that are associated with shear along the San Andreas transform fault system west of the volcanic field. Thus, they invoked three different mechanisms to explain the formation of the listric fault and some of the vent alignments documented during their analysis: an increase in Pinacate magma pressure, a decrease in the magnitude of the tectonic horizontal stresses, and a combination of both factors.

3. Methods

We analyzed the distribution of volcanism using the coordinates of 416 vents identified in El Pinacate by Lutz and Gutmann (1995). Examination of satellite images from this area allows the identification of a slightly larger number of vents (433), but the database of Lutz and Gutmann (1995) provides an associated age division for their vents, which is advantageous. Their age division is based on the degree of erosional modification as well as on stratigraphic relations observed both in stereo pairs and in the field. Due to the lack of more precise isotopic results for the majority of the vents in the field, that age division constitutes the best available information at present. Even if the broad age assignment is somewhat uncertain,

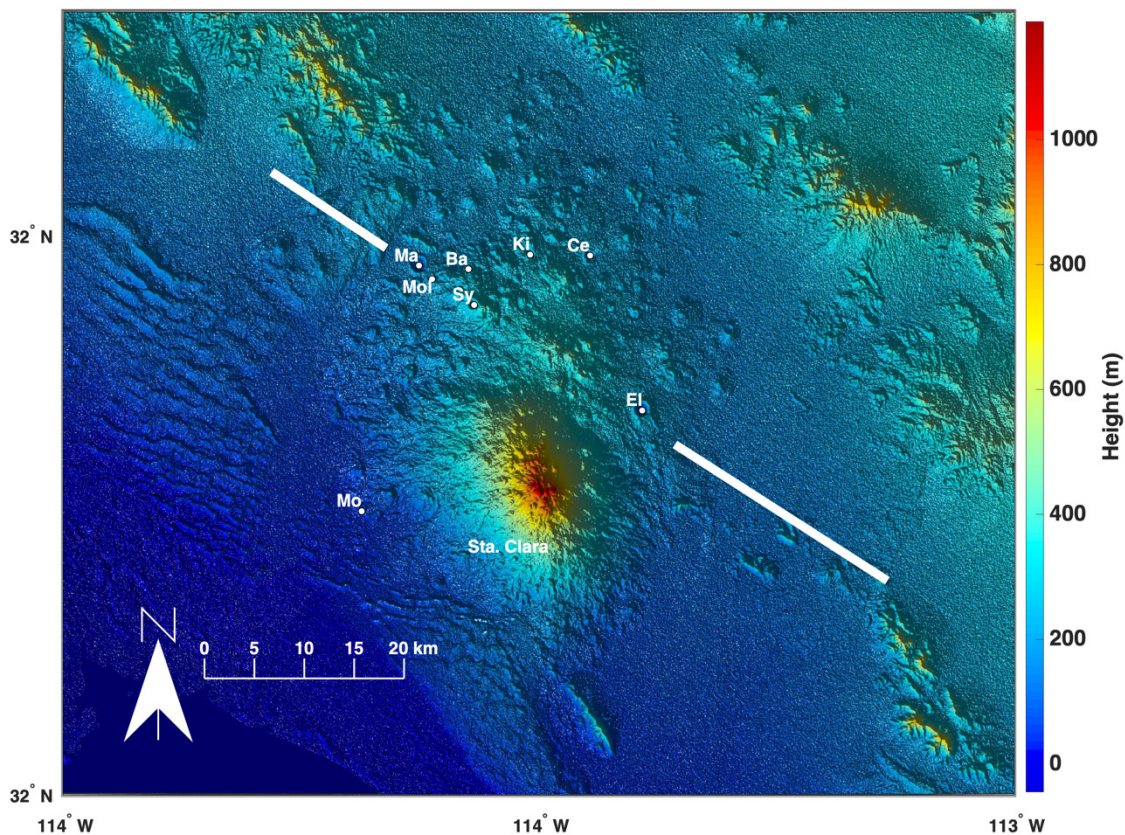


Figure 1 Digital Elevation Model of El Pinacate region. The eight maars in the volcanic field are shown for reference: Ba - Badillo Crater, Ce - Celaya Crater, El - Crater Elegante, Ki - Kino Crater, Ma - MacDougal Crater, Mo - Moon Crater, Mol - Molina Crater, Sy - Sykes Crater. The diagonal line marks the approximate location of the inferred listric fault mentioned by Lutz and Gutmann (1995).

it may capture general trends by focusing on the young (120 vents) vs. old (204 vents) classes, ignoring the intermediate / indeterminate age group (92 vents).

Aiming to overcome some of the biases and limitations of previous studies of the spatial distribution of vents in El Pinacate, we combined four methods: 1) a Gaussian kernel to generate a sequence of Probability Density Functions (PDFs), 2) the combination of several clustering methods to form the so called core-groups (Cañón-Tapia, 2020), 3) two-point azimuth analysis with a restriction of vent distance (Cebriá *et al.*, 2011), and 4) a hierarchical classification based on a general definition of a cluster (Cañón-Tapia, 2021a). All four methods were implemented using MATLAB codes. Brief descriptions of each method are as follows:

3.1. SEQUENCE OF PDFS USING A GAUSSIAN KERNEL

This method was used to some extent by Lutz and Gutmann (1995). Nevertheless, the PDFs that they showed were not systematically presented for the different age groups, nor were they presented in direct combination with the results of the other methods of analysis. The PDFs associated by a Gaussian kernel are defined by:

$$f(x, y) = \frac{1}{2\pi N C_n^2} \sum_{i=1}^N \exp\left(-\frac{1}{2} \left[\frac{d_i}{C_n}\right]^2\right) \quad (1)$$

where d_i is the distance between the point where the function is being determined and the i -th observation, N is the total number of observations (vents), and C_n is the smoothing factor. In this work, the distance between two points was calculated from the latitude-longitude coordinates assuming a sphere with radius equal to 6371 km. Several PDFs were calculated using values of C_n in the range 0.9 to 10 km. All the PDFs were normalized, so that contour lines were drawn at 10% intervals relative to the maximum probability-density of each function (f_{max}). The general location of the local maxima on the sequence of PDFs was used later as a guide to constrain the

probable number of clusters to be expected when completing the identification of core-groups.

3.2. CORE GROUPS

The basis for the identification of core groups is the use of more than one method of analysis leading to a more robust result than the identification of a given partition through the use of a single clustering method. This approach has been shown to yield partitions that are more compatible with geology-based classifications in an area where clusters of different characteristics (shape and size of outline, number of total observations, density structure of the membership, etc.) co-exist (Cañón-Tapia, 2020). In essence, this part of the analysis consists of the identification of vents that belong to the same group according to more than one clustering algorithm (or their variants). To standardize the analysis, Cañón-Tapia (2020) used the following clustering methods: Hierarchical agglomerative with average, centroid, median and complete linking criteria; Partitioning k-means, Partitioning k-medoids, and a Gaussian mixture model that relies on the Expectation-Maximization algorithm. Details of each of those methods can be found on either the MATLAB documentation or more extensively on Everitt *et al.* (2011) and McLachlan and Peel (2000). In this work we used the same list of methods.

To implement the automatized search of core-groups it is necessary to have a previous estimate of the number of clusters to be expected. As is often the case, the number of clusters to be identified is ill-determined at the beginning of any study. To avoid as much as possible biases introduced by any pre-conceptions about the spatial structure of the data (or about the number of clusters), in this work we analyzed the core-groups defined by a range on the number of expected clusters. The range was determined by counting the number of local maxima identified in the previously obtained PDF sequence, as described in the previous section. Once the specified number of core-groups had been identified, comparison between the location of the kernel-associated maxima and the core-groups allowed the identification of the most

stable groups. Regardless of such stability, a final decision concerning which groups should be considered as more likely to be geologically significant was postponed until two additional methods of analysis were completed.

3.3. A HIERARCHICAL DEFINITION OF POSSIBLE CLUSTERS

The approach adopted here relies on the comparison of two distances that can be used to define a cluster. One of those distances is the largest distance between one arbitrary object belonging to one cluster and its nearest neighbor within that cluster (hereafter referred to as the maximum within cluster distance, or MWCD). The other distance to be calculated is the shortest distance between one arbitrary object belonging to the cluster and any one object outside of that cluster (hereafter referred as the between cluster distance, or BCD). It is remarked that the BCD only requires members of one cluster to be identified because the observations outside that cluster may or may not belong to a second cluster. MWCD allows us to separate a tentative membership related with a zone of interest (as for example a zone with large number of vents/area). Another advantage is that the search for clusters can be made hierarchically (for example, the cluster with the largest local density is defined first, regardless of the total number of clusters or the characteristics of any other possible cluster in the entire population) allowing identification of overlapping and sub-clustering structures after all the observations have been assigned to their corresponding groups. A third advantage is that it is possible to leave some observations without an associated group, which is useful in cases of chaining effects or extreme overlapping.

To make the search in a systematic form, we adopted the same protocol as described in Cañón-Tapia, E. (2021a).

3.4. SHORT-DISTANCE VENT ALIGNMENTS

Interpretation of patterns of vent distribution commonly assume that magma reaches the surface through vertical conduits having horizontal

dimensions not much larger than the lateral extension of the vent at the surface in at least one direction (Valentine and Perry, 2006). The extension of the conduit in a perpendicular direction may be much larger than one single vent, potentially feeding more than one eruption along a line of vents that may extend for tens of kilometers like

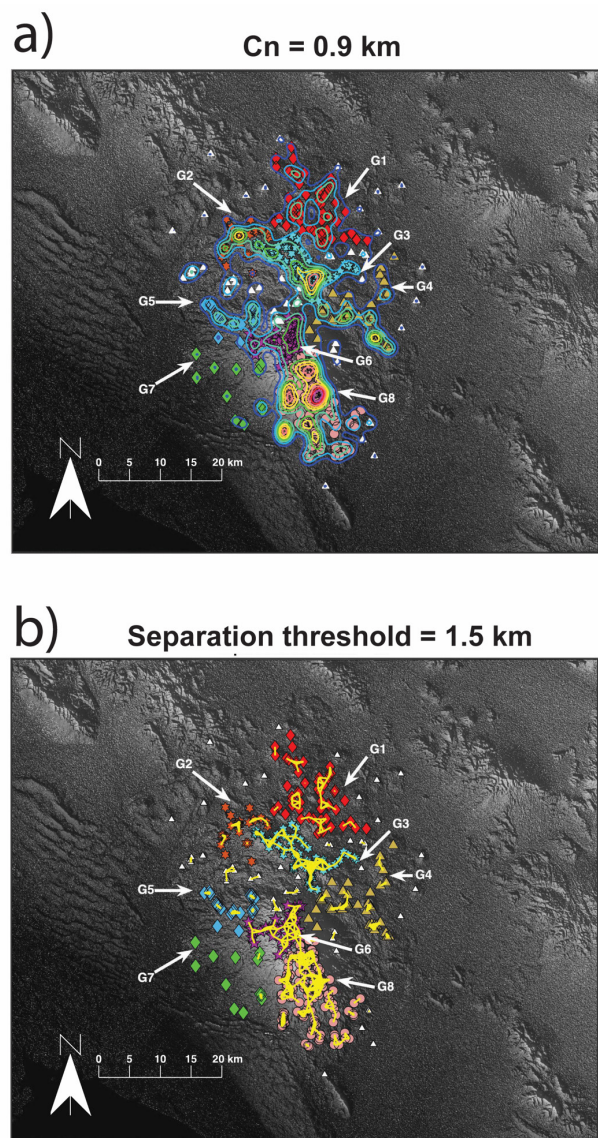


Figure 2 Method comparison. a) 8 core-groups superimposed to PDF obtained with $C_n=0.9$ km. b) 8 core-groups and lines joining vents that are separated by less than 1.5 km. Vents belonging to each of the 8 main core-groups are identified by a different symbol and color; those not associated with any of the core-groups are shown as white triangles. The arrows and labels allow the identification of those groups with the distances presented in Table 1.

the Skaftár Fires eruption, Iceland, in 1783-1785 (Thordarson and Self, 1993). Regardless of the extension of the feeding conduit, the separation of vents that have been fed by the same dyke has been documented to be less than 1.5 km (Tibaldi, 1995). Consequently, we adapted the two-point azimuth method used to find vent alignments with a separation limit (Cebriá *et al.*, 2011) to search for those vents more likely to have been fed by a common intrusion in El Pinacate region. The idea is that drawing in a map those segments that separate adjacent vents by a specified distance (always smaller or equal to 1.5 km) might reveal underlying structures such as rift zones in shield volcanoes, or interconnections with a central conduit in a very straightforward manner. The information provided by the location of plexus defined by a large number of short-distance vent segments is therefore probably linked to the presence of conduits of magma that are more important within a volcanic system than the location of individual vents.

4. Results

Figure 2 allows visual comparison of the results of methods 1 to 3, and the results of the fourth method are reported in Table 1. The first three methods support the identification of eight groups of vents, although their boundaries are not well established. Attempts to identify independent clusters that could be separated from their neighbors by a distinctive Between Cluster Distance (BCD) almost invariably led to the merging of two or more of the adjacent core-groups, therefore indicating that in most cases the separation between groups is ill-defined. Allowing for the isolation of intermediate vents that promote chaining effects that result in the union of adjacent clusters, the Mean Within Cluster Distance (MWCD) and BCD of the updated core-groups was calculated (Table 1). In this form, the boundaries of the groups is easier to define.

In both panels of Figure 2 the north half of El Pinacate field is divided in two dominant groups

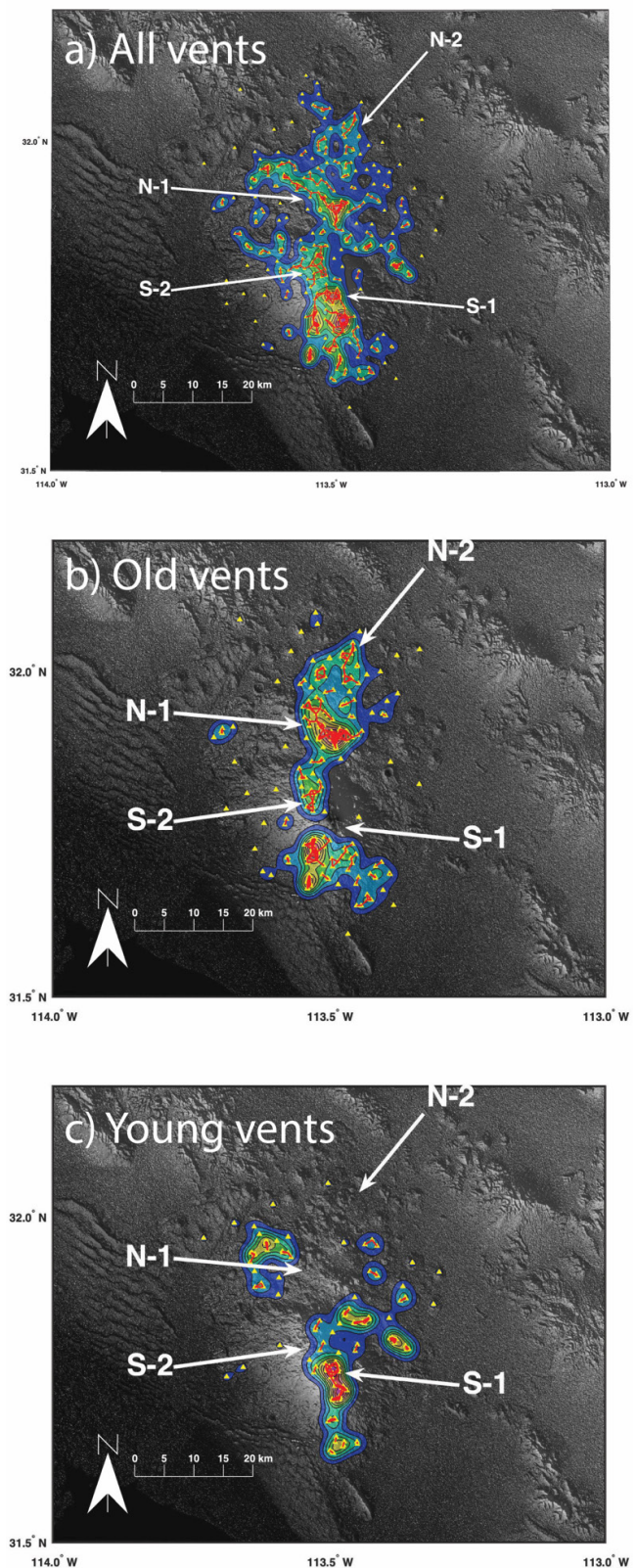


Figure 3 Location of the four main structures identified in El Pinacate. Vents separated by less than 1.25 km are joined by a red line. a) all vents, b) old vents, c) young vents.

Table 1. Maximum Within Cluster Distances (MWCD) – diagonal, and Between Cluster Distances (BCD) – off-diagonal of the 8 groups identified in El Pinacate region. All distances are in km.

	G1	G2	G3	G4	G5	G6	G7	G8
G1	2.1	2.2	1.6	5.0	14.1	12.0	21.5	17.3
G2		3.0	1.7	12.7	5.5	9.2	14.9	15.7
G3			1.1	1.6	7.9	3.3	13.4	8.3
G4				2.8	8.9	2.0	9.6	2.2
G5					2.9	1.7	4.3	9.3
G6						1.3	1.8	1.5
G7							4.2	3.3
G8								1.4

(G1 and G3), G3 having a marked NW-SE elongation. The southern half of the field is dominated by groups G6 and G8, although the separation between them is not straightforward. The other four groups seem to be peripheral and have a subordinate character. Focusing attention of the four dominant groups, Figure 3 shows their position and associated vents divided by age.

5. Discussion

5.1. AGE CONSTRAINTS

In terms of age, each of the eight groups includes both young and old vents, therefore precluding an interpretation involving a systematic migration of volcanic activity. Nevertheless, the distribution of volcanic vents over the entire area seems to have experienced some changes with age. Older vents tended to be arranged in a North-South band (Figure 3b) whereas more recent volcanism took place parallel to the inferred listric fault that crosses the field at its middle section, especially within the boundaries of G2, G4 and G5. In terms of the four dominant groups, the plexuses of vents can be tentatively associated to central systems arranged along a N-S line across the entire field. Nevertheless, N-1 is the only having an orientation parallel to the trend of the inferred fault. Considering the ages of volcanism (< 1.7 Ma) and the most probable age of the listric fault (~ 5 Ma), a change in the orientation of the tectonic stress

after volcanism had started is an unlikely explanation for the shape of N-1. If such a reorientation of stress had occurred, it would have affected all younger vents, and not only those at the boundaries of the groups of vents that are spatially closer to the inferred listric fault.

5.2. DEPTH OF MAGMA SOURCE

Following Cañón-Tapia (2021a) and Cañón-Tapia (2021b) we calculate independent PDF contours for each of the four dominant groups to constraint minimum depths of magma for each group. Results are shown in figure 4, implying a minimum magma depth between 7 and 14 km. This depth agrees well with estimates to the regional depth to the Curie isotherm (Campos-Enriquez *et al.*, 2019), and with the presence of mafic rocks of gabbroic composition (García-Abdeslem, 2020). It must be noted that the range in depth obtained with this method in Kamchatka range between 3 and 8 km (Cañón-Tapia, 2021b) and on Jeju island range between 5 and 35 km (Cañón-Tapia, 2021a). Consequently, even when many volcanoes may have reservoirs on the range 7-14 km, the result obtained here is specific for El Pinacate and not a generic assertion valid for any volcano around the world.

5.3. EL PINACATE FOUR SHIELD VOLCANOES

Our four dominant groups coincide remarkably well with the three shield volcanoes proposed by Donnelly (1974). Donnelly's southern shield

coincides with the Santa Clara edifice (S-1 and S-2), his central shield coincides with our N-1 structure, and his north shield roughly corresponds with our N-2 structure (although according to Donnelly, this shield includes only the north part of structure N-2 and extends much farther to the north of the field). The extent of the main part of the four shields proposed here is shown in figure 5. Each shield is characterized by having its own centralized system from which other vents emanate, while remaining identifiable as independent edifices regardless of their relative topographical expression. This description is reminiscent of the description of a “volcanic-shield cluster” proposed by Wentworth and Macdonald (1953).

From a broader perspective, the distribution of vents on S-1 and N-2 resemble the overall vent distribution observed at Olympus Mons if each is regarded independently. Also, the general distribution of vents in El Pinacate has some broad similarities with the distribution of vents observed in two lunar shields (Marius Hills and Mons Rumker)

(Jacobo-Bojórquez and Cañón-Tapia, 2020). For these reasons, we consider that El Pinacate can be visualized as a variant of a shield-cluster in which the topographic expression of each shield is not as clear as in Hawai'i, in which crustal structures have influenced mainly the development of one of those shields.

5.4. TECTONIC SIGNIFICANCE

The location of El Pinacate volcanic field in the vicinity of a tectonically controlled rifted basin is somewhat reminiscent of the relationship that exists between the Al Haruj volcanic province and the Sirt basin in central Lybia (Elshaafi and Gudmundsson, 2016; Elshaafi and Gudmundsson, 2017). Nevertheless, it is not clear whether El Pinacate can be considered to be within the limits of the tectonically controlled basin or not, whereas at the Al Haruj Province the volcanic field is clearly within the limits of the Sirt basin. This would explain the differences in vent distribution at both sites. Vent distribution at the Al Haruj Province is

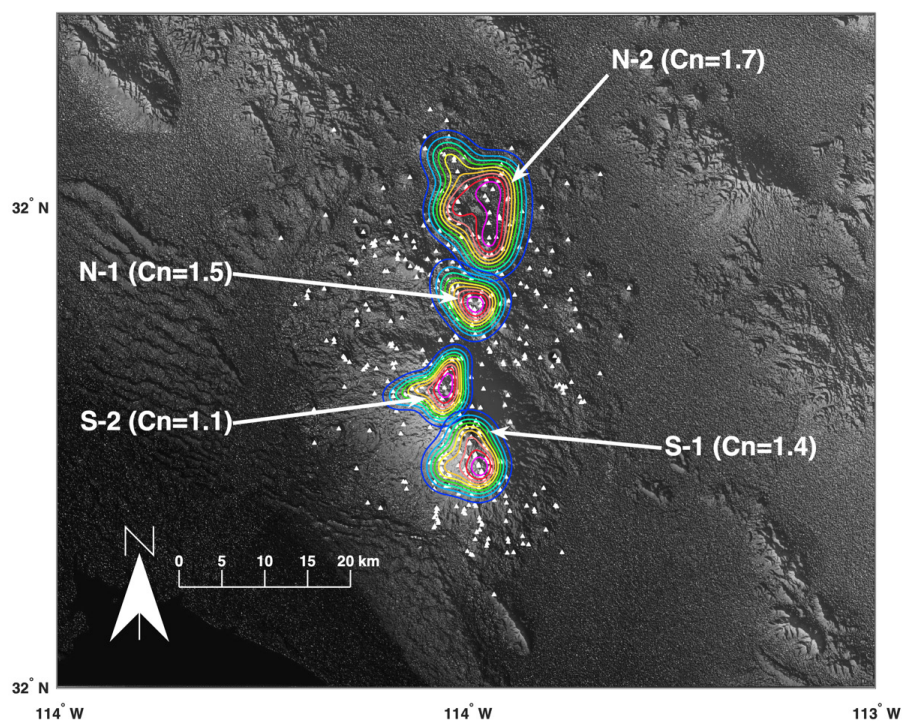


Figure 4 PDF contours calculated for the vents of each main structure independently of the others. The used Cn is indicated on each case.

markedly controlled by underlying fissures leading to very prominent vent alignments, whereas at El Pinacate such alignments are not dominant at all. Also, even when it can be considered that there is a clear morphological distinction between the north and south halves of the El Pinacate region, this is related to the presence of a larger structure on the south (Sta. Clara large-shield volcano) whereas at the Al Haruj Province the difference between north and south is related to the size and general characteristics of individual vents (larger lava shields on the north vs. smaller cones in the south).

Despite those differences, in both places it is possible to identify more than one independent volcanic system, each probably related to its own set of magma reservoirs from which the magma feeding the vents at the surface is temporarily stored.

Our interpretation explains the N-S elongation and vent alignment noted by Lutz and Gutmann

(1995), as well as the dominant N20W° vent alignment. Unlike previous interpretations, ours indicate that the overall N-S shape of El Pinacate volcanic field is due to an elongated integrated magma source that includes a combination of reservoirs at various depths, but that is controlled by the regional gradient of temperatures, whereas the N20°W vent alignment is due to the influence of the listric fault on just one of the main shields. The distribution of vents surrounding those main shields results from the combined effect of the independent magma reservoirs and the crustal structures.

Identification of the main groups is a useful guide for future research on El Pinacate because they justify focusing future field work on one of those structures at a time. Adoption of such a work plan is likely to yield results that could be used to assess the geologic significance of the proposed structures in more efficiently than until now.

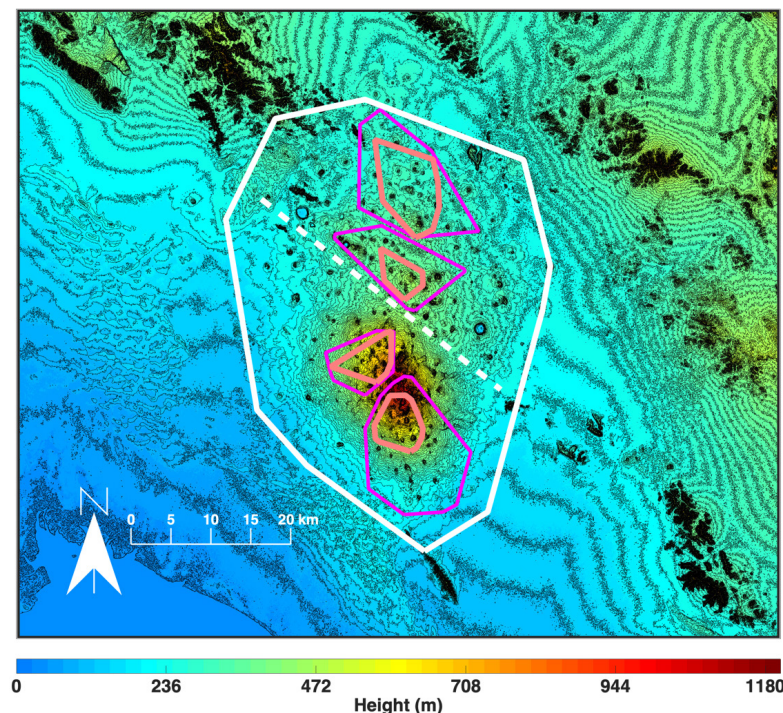


Figure 5 Topographic map of El Pinacate region. The envelope of the vents (convex-hull) is shown for all the field (white line), each of the four main structures (magenta line) and the vents associated to a possible central conduit (orange lines). The dashed white line marks the approximate position of the trace of the listric fault.

Contributions of authors

Both authors equally participated in the following activities: conceptualization, analysis or data acquisition, methodologic-technical development, writing of the original manuscript, writing of the corrected and edited manuscript.

Financing

Proyecto CONACYT A1-S-23107, technical manager, E. Cañón Tapia.

Acknowledgements

The comments of anonymous reviewers, A. Elshaafi and K. Németh to an old version of this work are appreciated. Special thanks are due to J. Guttmann for providing us with a copy of the dissertation of Donnelly and numerous comments made to several versions of this work.

Conflicts of interest

The authors declare that they have no conflict of interest

References

Alva Valdivia, L.M., Rodríguez-Trejo, A., Vidal-Solano, J., R., Paz-Moreno, F., Agarwal, A., 2019, Emplacement temperature resolution and age determination of Cerro Colorado tuff ring by paleomagnetic analysis, El Pinacate volcanic field, Mexico: *Journal of Volcanology and Geothermal Research*, 369, 145-154. <https://doi.org/10.1016/j.jvolgeores.2018.11.012>

Campos-Enriquez, J.O., Espinosa-Cardena, J.M., Oksum, E., 2019, Subduction control on the curie isotherm around the Pacific-North America plate boundary in northwestern Mexico (Gulf of California). Preliminary

results: *Journal of Volcanology and Geothermal Research*, 375, 1-17. <https://doi.org/10.1016/j.jvolgeores.2019.03.005>

Cañón-Tapia, E., 2020, Influence of method selection on clustering analyses of point-like features: Examples from three zones of distributed volcanism: *Geomorphology*, 354, 107063. <https://doi.org/10.1016/j.geomorph.2020.107063>

Cañón-Tapia, E., 2021a, Vent distribution on Jeju Island, South Korea: Glimpses into the subvolcanic system: *Journal of Geophysical Research: Solid Earth*, 126, e2021JB022269. <https://doi.org/10.1029/2021JB022269>

Cañón-Tapia, E., 2021b, Volcano distribution and Tectonics: A Planetoidic Perspective, in Foulger, G.R., Hamilton, C., Jurdy, D.M., Stein, C.A., Hamilton, L.C., Howard, K., Stein, S., (Eds.), *In the Footsteps of Warren B. Hamilton: New Ideas in Earth Science: Geological Society of America, Special paper 553*, 83-93. [https://doi.org/10.1130/2021.2553\(08\)](https://doi.org/10.1130/2021.2553(08))

Cañón-Tapia, E., Jacobo-Bojorquez, R.A., 2022, Sub-Volcanic Structure Beneath Marius Hills, Moon, Inferred From Vent Distribution: *Journal of Geophysical Research: Planets*, 127, e2021JE006960. <https://doi.org/10.1029/2021JE006960>

Cebriá, J.M., Martín-Escorza, C., López-Ruiz, J., Morán Zenteno, D.J., Martiny, B.M., 2011, Numerical recognition of alignments in monogenetic volcanic areas: Examples from the Michoacán-Guanajuato Volcanic field in Mexico and Caltrava in Spain: *Journal of Volcanology and Geothermal Research*, 201, 73 - 82. <https://doi.org/10.1016/j.jvolgeores.2010.07.016>

Donnelly, M.F., 1974, *Geology of the Sierra del Pinacate Volcanic Field, Northern Sonora, Mexico and Southern Arizona: USA*, Stanford University, tesis doctoral, 722 pp.

Elshaafi, A., Gudmundsson, A., 2016, Volcanotectonics of the Al Haruj Volcanic Province, Central Libya: *Journal of Volcanology and*

- Geothermal Research, 325, 189-202. <https://doi.org/10.1016/j.jvolgeores.2016.06.025>
- Elshaafi, A., Gudmundsson, A., 2017, Distribution and size of lava shields on the Al Haruj al Aswad and the Al Haruj al Abyad Volcanic Systems, Central Libya: *Journal of Volcanology and Geothermal Research*, 338, 46-62. <https://doi.org/10.1016/j.jvolgeores.2017.03.012>
- Everitt, S., Landau, S., Leese, M., 2011, *Cluster analysis*: London, Wiley.
- García-Abdeslem, J., 2020, On the relationship between volcanic pointlike features and the crust-mantle boundary at the Pinacate Volcanic Field, Sonora, México: *Journal of South American Earth Sciences*, 104, 102808. <https://doi.org/10.1016/j.jsames.2020.102808>
- García-Abdeslem, J., Calmus, T., 2015, A 3D model of crustal magnetization at the Pinacate Volcanic Field, NW Sonora, Mexico: *Journal of Volcanology and Geothermal Research*, 301, 29-37. <https://doi.org/10.1016/j.jvolgeores.2015.05.001>
- Gutmann, J., T., 2002, Strombolian and effusive activity as precursors to phreatomagmatism: eruptive sequence at maars of the Pinacate volcanic field, Sonora, Mexico: *Journal of Volcanology and Geothermal Research*, 113, 345-356. [https://doi.org/10.1016/S0377-0273\(01\)00265-7](https://doi.org/10.1016/S0377-0273(01)00265-7)
- Gutmann, J.T., 2007, Geologic studies in the Pinacate: *Journal of the Southwest*, 49, 189-243. <https://doi.org/10.1353/jsw.2007.0004>
- Ives, R.L., 1942, The discovery of Pinacate volcano: *The Scientific Monthly*, 54, 230-237.
- Jacobo-Bojórquez, R.A., Cañón-Tapia, E., 2020, Distribution of Eruptive Centers on Top of Large Shield Volcanoes in the Inner Solar System: General Classification and Glimpses of Their Subvolcanic Structure: *Journal of Geophysical Research: Planets*, 125, e2020JE006431. <https://doi.org/10.1029/2020JE006431>
- Le Corvec, N., Bernhard Spörli, K., Rowland, J., Lindsay, J., 2013, Spatial distribution and alignments of volcanic centers: Clues to the formation of volcanic fields: *Earth-Science Reviews*, 124, 96 - 114. <https://doi.org/10.1016/j.earscirev.2013.05.005>
- Lutz, M.T., Gutmann, J.T., 1995, An improved method for determining and characterizing alignments of point like features and its implications for the Pinacate volcanic field, Sonora, Mexico: *Journal of Geophysical Research*, 100, 17659 - 17670. <https://doi.org/10.1029/95JB01058>
- Lynch, D.J., 1991, Pinacate's largest lava flow: *CEDO News*, 4, 1-13.
- Lynch, D.J., Musselman, T.E., Gutmann, J.T., Patchett, P.J., 1993, Isotopic evidence for the origin of Cenozoic volcanic rocks in the Pinacate volcanic field, northwestern Mexico: *Lithos*, 29, 295-302. [https://doi.org/10.1016/0024-4937\(93\)90023-6](https://doi.org/10.1016/0024-4937(93)90023-6)
- Lynch, D.J.II, 1981, Genesis and geochronology of alkaline volcanism in the Pinacate volcanic field northwestern Sonora, Mexico: The University of Arizona, tesis doctoral, 248 p.
- Martin, U., Nemeth, K., 2004, Eruptive mechanism of phreatomagmatic volcanoes from the Pinacate Volcanic Field: Comparison between Crater Elegante and Cerro Colorado, Mexico: *Second International Maar Conference: Hungary, Geological Institute of Hungary*, 75p.
- McLachlan, G., Peel, D., 2000, *Finite mixture models*: Hoboken, NJ, John Wiley & Sons, Inc.
- Rodríguez-Trejo, A., Alva Valdivia, L.M., Vidal-Solano, J.R., 2019, Paleomagnetism and rock magnetic properties of Late Pleistocene volcanism from El Pinacate volcanic field, northwest Mexico: *Journal of South American Earth Science*, 96, 102368. <https://doi.org/10.1016/j.jsames.2019.102368>
- Sumner, J.R., 1972, Tectonic significance of gravity and aeromagnetic investigations at the head of the Gulf of California:

- Geological Society of America, Bulletin, 83, 3103-3120. [https://doi.org/10.1130/0016-7606\(1972\)83\[3103:T SOGAA\]2.0.CO;2](https://doi.org/10.1130/0016-7606(1972)83[3103:T SOGAA]2.0.CO;2)
- Thordarson, T., Self, S., 1993, The Laki (Skaftár Fires) and Grímsvötn eruptions in 1783–1785: Bulletin of Volcanology, 55, 233–263. <https://doi.org/10.1007/BF00624353>
- Tibaldi, A., 1995, Morphology of pyroclastic cones and tectonics: Journal of Geophysical Research, 100(24), 521-535. <https://doi.org/10.1029/95JB02250>
- Turrin, B.D., Gutmann, J.T., Swisher, C.C. III, 2008, A 13 ± 3 ka age determination of a tholeiite, Pinacate volcanic field, Mexico, and improved methods for $^{40}\text{Ar}/^{39}\text{Ar}$ dating of young basaltic rocks: Journal of Volcanology and Geothermal Research, 177, 848-856. <https://doi.org/10.1016/j.jvolgeores.2008.01.049>
- Valentine, G.A., Perry, F.V., 2006, Decreasing magmatic footprints of individual volcanoes in a waning basaltic field: Geophysical Research Letters, 33(14), L14305. <https://doi.org/10.1029/2006GL026743>
- Wadge, G., Cross, A.M., 1989, Identification and analysis of the alignments of point-like features in remotely-sensed imagery. Volcanic cones in the Pinacate volcanic field, Mexico: International Journal of Remote Sensing, 10, 455-474. <https://doi.org/10.1080/01431168908903885>
- Wentworth, C.K., Macdonald, G.A., 1953, Structures and forms of basaltic rocks in Hawaii. United States Geological Survey, 98 p.
- Zawacki, E.E., Clarke, A.B., Arrowsmith, J.R., Bonadonna, C., Lynch, D.J., 2019, Tecolote volcano, Pinacate volcanic field (Sonora, Mexico): A case of highly explosive basaltic volcanism and shifting eruptive styles: Journal of Volcanology and Geothermal Research, 379, 23-44. <https://doi.org/10.1016/j.jvolgeores.2019.04.011>